

Original Article

Implications of Simulation of CO₂ Dispersion on Marine Potential Environmental Impact Assessment and Monitoring at CO₂ Storage Sites

Keisuke Uchimoto ^{a,b}, Yuji Watanabe ^{a,b}, Kazuhiro Misumi ^c, Takaki Tsubono ^c, Daisuke Tsumune ^c, Jiro Suekuni ^{a,b}, Ziqiu Xue ^{a,b}

^a Geological Carbon Dioxide Storage Technology Research Association, Kizugawa, Japan

^b CO₂ Storage Research Group, Research Institute of Innovative Technology for the Earth, Kizugawa, Japan

^c Central Research Institute of Electric Power Industry, Abiko, Japan

ABSTRACT

When carbon dioxide (CO₂) is stored in sub-seabed geological formations, the environmental impact assessment assuming CO₂ leakage and monitoring CO₂ concentration in the sea are mandatory in Japan. The marine environment is not impacted by CO₂ storage itself but by the unlikely event of leakage. Thus, it is referred to as potential environmental impact assessment (PEIA). We conducted an ocean simulation for Hidaka Bay off Hokkaido, releasing passive tracers regarded as leaked CO₂. Biological impact data were newly compiled, and 4 thresholds for biological impacts depending on both the increase in partial pressure of CO₂ (pCO₂) and exposure time were set. The increase in pCO₂ estimated in the simulation, assuming CO₂ leak rates of 1,000 tonnes/y and 10,000 tonnes/y, exceeded no thresholds. The tracer concentration became almost equilibrium within about a week after the commencement of the release, and the increase in pCO₂ was much larger in summer than winter. These results suggest that the simulation of leaked CO₂ for PEIA be run for about a month in summer, and that monitoring CO₂ concentration be also conducted in summer. It is also implied that monitoring pCO₂ could detect leakage at O(10⁴) tonnes/y or larger than it.

Keywords: CCS, geological CO₂ storage, biological impact, environmental impact assessment, simulation

INTRODUCTION

Carbon dioxide (CO₂) emissions have increased since the Industrial Revolution. The concentration of CO₂ in the atmosphere has, consequently, increased from around 280 parts per million (ppm) before the Industrial Revolution to around 410 ppm in 2019 [1]. The increase in the atmospheric CO₂ concentration is a primary contributor to global warming. It has been widely recognized that CO₂ emissions should be reduced, and many countries, including Japan, have declared that they aim to achieve net zero greenhouse gas emissions by around 2050.

To achieve the net zero emissions, CO₂ capture and storage

(CCS) is considered essential [2]. In CCS, CO₂ captured at large point sources is stored in deep geological formations such as saline aquifers and depleted oil and gas reservoirs. While the formations suitable for CO₂ storage are distributed both onshore and offshore, we focus here on offshore storage partly because some countries including Japan, Korea, Norway, and the United Kingdom focus on offshore CO₂ storage because of the limited inland space [3], and partly because a lot of potential storage reservoirs for gigatonne-scale CO₂ storage are located under offshore continental shelves and so “the offshore settings offer both significant volumes and practical deployment benefits at scale” [4].

Leakage is one of the public concerns about geological CO₂

Corresponding author: Keisuke Uchimoto, E-mail: uchimoto@rite.or.jp

Received: March 30, 2023, Accepted: July 26, 2023, Published online: October 10, 2023

 **Open Access** This is an open-access article distributed under the terms of the Creative Commons Attribution Non-Commercial No Derivatives (CC BY-NC-ND) 4.0 License. <http://creativecommons.org/licenses/by-nc-nd/4.0/>

storage (*e.g.*, [5,6]) although the formations for CO₂ storage are carefully selected so that CO₂ can be stored safely and stably in the reservoir; several trap mechanisms prevent the stored CO₂ from escaping from the reservoir [7]. In the event of CO₂ leakage from offshore reservoirs, most of leaked CO₂ would not directly return to the atmosphere but would dissolve into seawater (*e.g.*, [8]), depending on conditions such as the leak rate, the water depth, water temperature, and so on. This is preferable from the standpoint of the atmospheric CO₂ reduction but may have impact on marine organisms.

Thus, marine environmental impact assessment (EIA) assuming CO₂ leakage before the injection is necessary to gain social acceptance, and such an EIA is also mandatory in many countries based on the London Protocol [9]. In Japan, Act on Prevention of Marine Pollution and Maritime Disaster stipulates the legal requirement for EIA, as well as marine monitoring during and after the injection [10,11]. It is noted that there is an important difference between this marine EIA and the usual EIA. While impacts by the project itself, *e.g.* operation of the project and construction of facilities, are assessed in the usual EIA, impacts in the unlikely event of CO₂ leakage are assessed in the marine EIA for offshore CO₂ storage and, therefore, it is referred to as potential environmental impact assessment (PEIA [11]). To assess the impact of CO₂ leakage on marine environment, the increase in CO₂ concentration in seawater due to leakage need to be predicted. Numerical simulations are an effective method for it (*e.g.*, [3,12–14]). Some studies (*e.g.*, [3,13]) used a tidal-current model, which were forced by only tidal forcing. Such a model is unsuitable for a simulation of sea areas where ocean currents exert a great influence on the flow fields. Hidaka Bay in Japan (Fig. 1), under which CO₂ has been stored in the Tomakomai CCS Demonstration Project, is one of those areas. The coastal flow of Hidaka Bay is greatly influenced by the Coastal Oyashio, the Tsugaru Warm Current, and flow forced by a monsoon wind [15] while the tidal current is weak [16]. Thus, to simulate dispersion of the leaked CO₂ in Hidaka Bay, an ocean model representing those currents and flows is necessary.

In the present study, we conduct a simulation of passive tracers regarded as leaked CO₂ from off Tomakomai in Hidaka Bay keeping the PEIA before the CO₂ injection in mind. Simulations for the PEIA ought to be clearly distinct from simulations that would be conducted to predict leaked CO₂ dispersion if CO₂ were to leak. In the latter simulations, there would be many known conditions, *e.g.* the leakage point(s) and possibly the leakage rate, and to some extent correct and concrete results would be expected (*i.e.*, where, when and

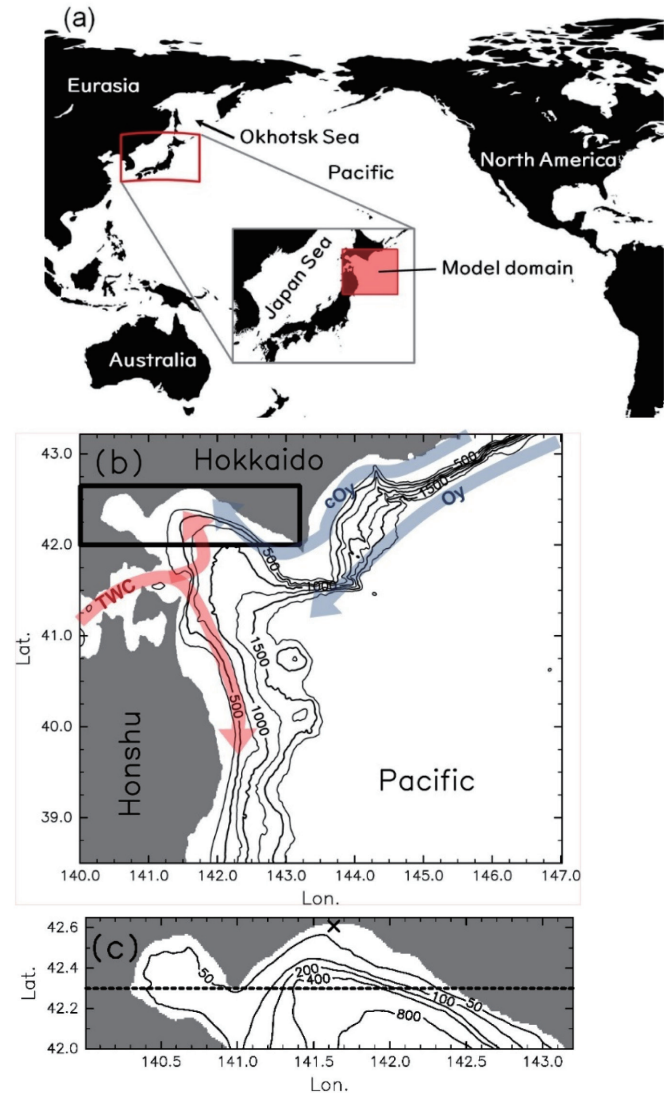


Fig. 1 Model domain is denoted with a red rectangular in (a), and is enlarged in (b). The rectangular in (b) denotes Hidaka Bay and is enlarged in (c). Contour lines in (b) and (c) represents depth. The cross in (c) denotes the release point of the tracers. The map around the Japan Islands (the inset in (a)) was based on the data of Smith and Sandwell [61]. In (b), the Tsugaru Warm Current (TWC), the coastal Oyashio (cOy) and the Oyashio (Oy) are schematically shown.

how much CO₂ concentration would be). By contrast, in the former simulations, all the conditions and leakage scenarios are assumed, and so too detailed or too concrete results based on specific assumptions may be sometimes meaningless or pointless.

To assess biological impacts of CO₂ concentration predicted by the simulation, biological impact thresholds are necessary. Although some studies used the thresholds consisting

of only changes in a CO₂ concentration index such as partial pressure of CO₂ (pCO₂) and pH (*e.g.*, [3,13]), biological impacts depend not only on CO₂ concentration but also on its duration of exposure [17]. We have newly compiled biological impact data and set thresholds depending on increase of pCO₂ (Δ pCO₂) and its duration.

Lastly, we sum up the implications for the PEIA and marine monitoring for offshore CO₂ storage, including, for example, the most suitable season to monitor a CO₂ concentration index if it is monitored only once a year, as the Japanese act requires to monitor chemical property of seawater (*i.e.*, a CO₂ concentration index) at least once a year.

MATERIALS AND METHODS

Ocean model

We employed an ocean model developed at the Central Research Institute of Electric Power Industry (CRIEPI), based on the Regional Ocean Modeling System, which is a free-surface, terrain-following, hydrostatic primitive equations ocean model [18]. The present model setup is similar to that of the Fukushima offshore model of CRIEPI, which was used for the assessment of the Fukushima Dai-ichi Nuclear Power Plant accident [19]. The Multidimensional Positive Definite Advection Transport Algorithm (MPDATA [20]) was used. The harmonic horizontal viscosity and diffusion coefficient were 50 m²/s and 10 m²/s, respectively. K-profile parameterization [21] were used for the vertical mixing. The model domain spans 140°–147°E and 38.5°–43.2°N (Fig. 1). Horizontal grid resolution is 1/120°, which is equivalent to about 700 m and 900 m in zonal and meridional directions, respectively. There are 45 layers in the vertical. While the layer heights vary from point to point because of the terrain-following coordinate, an example of the layer heights is shown in Table 1. The maximum depth in the model is set at 2,000 m to reduce the computer resources (Fig. 1b).

The model was integrated for 1 year from the quiescent state with the temperature and salinity fields based on the Japan Coastal Ocean Prediction Experiment 2 (JCOPE2) reanalysis data [22] on 1st March 2011, forced at the sea surface by wind stress, and heat and freshwater fluxes from the Numerical Weather Forecasting and Analysis System ([23]). Daily river discharged data from a model called HYDREEMS [24] were applied to grid cells of river mouths. Tidal data of 8 components (M₂, S₂, N₂, K₂, K₁, O₁, P₁, and Q₁) of TPXO7 [25] were given along the open lateral boundaries so that tidal oscillations were reasonably reproduced in the model domain (Fig. 2). To represent mesoscale eddies,

Tabel 1 The height of each layer at the tracer release point.

| Layer number (1: bottom, 45: surface) | Height [m] |
|---------------------------------------|------------|
| 45 | 0.08 |
| 44 | 0.08 |
| 43 | 0.08 |
| 42 | 0.08 |
| 41 | 0.08 |
| 40 | 0.08 |
| 39 | 0.08 |
| 38 | 0.09 |
| 37 | 0.09 |
| 36 | 0.09 |
| 35 | 0.09 |
| 34 | 0.10 |
| 33 | 0.10 |
| 32 | 0.10 |
| 31 | 0.11 |
| 30 | 0.12 |
| 29 | 0.12 |
| 28 | 0.13 |
| 27 | 0.14 |
| 26 | 0.15 |
| 25 | 0.16 |
| 24 | 0.17 |
| 23 | 0.19 |
| 22 | 0.21 |
| 21 | 0.23 |
| 20 | 0.25 |
| 19 | 0.28 |
| 18 | 0.31 |
| 17 | 0.34 |
| 16 | 0.38 |
| 15 | 0.42 |
| 14 | 0.48 |
| 13 | 0.53 |
| 12 | 0.60 |
| 11 | 0.68 |
| 10 | 0.76 |
| 9 | 0.86 |
| 8 | 0.98 |
| 7 | 1.11 |
| 6 | 1.26 |
| 5 | 1.43 |
| 4 | 1.62 |
| 3 | 1.84 |
| 2 | 2.09 |
| 1 | 2.38 |

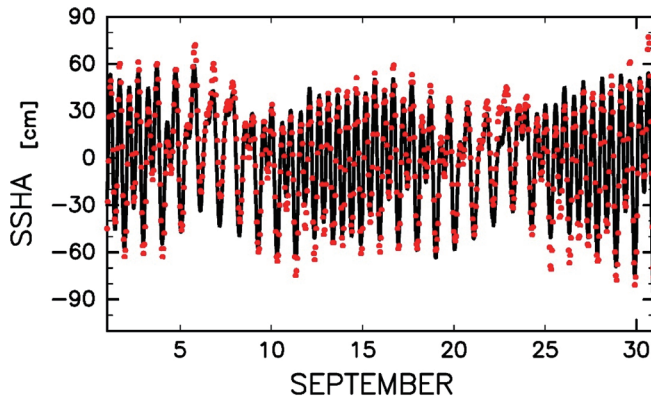


Fig. 2 Sea surface height anomaly (SSHA) from the monthly mean at the TOMAKOMAI-NISHIKO tide station, which is located at 42.63N, 141.6E. The red dots denote observed data and the black line denotes the simulated ones.

water masses and water systems, temperature and salinity were nudged to the JCOPE2 reanalysis data with the nudging parameter 1 day⁻¹, in all the domain except for Hidaka Bay (**Fig. 1c**), where the nudging was weakened toward the north from 42°N to 42.3°N, and was not applied northward of 42.3°N.

Release of passive tracers

Four passive tracers, regarded as leaked CO₂, were continuously released at a constant rate of 1 unit per year at the bottom cell at 42.61°N, 141.63°E (the cross in **Fig. 1c**; **Table 1**), the second grid point from the coast, under which the reservoir of the Tomakomai CCS Demonstration Project is located. The four tracers differed only in the start time of the release, which was 1st day of May, August, November 2011, and February 2012, respectively, and hereafter we refer to the tracers as dye01, dye02, dye03, and dye04, respectively.

Conversion of tracer concentration to ΔpCO₂

Increase in ΔpCO₂ is used as an index of biological impacts [26]. Regarding the concentration of the tracer as the increase in dissolved inorganic carbon (DIC) due to CO₂ leakage, we converted it into ΔpCO₂ using mocsy [27], in which the formulations for the dissociation constants of carbonic acid by Lueker *et al.* [28] and the formulation for the equilibrium constant for hydrogen fluoride by Dickson and Riley [29] were used. In the conversion, temperature and salinity calculated in the model were used, and the background DIC values were set at 2,093 μmol/m³, which were estimated from observed data [30]. Total alkalinity (*TA*

[mol/L]) was calculated using an empirical equation: *TA* = 46.29*S* + 747, where *S* is salinity [31]. Concentrations of total dissolved inorganic phosphorus and silicon were assumed to be 0. The leak rate is also necessary in the conversion, but the range of the leak rate to be discussed is unclear because CO₂ leakage from the sub-seabed geological CO₂ storage has never occurred, and also because geological formations that could stably retain CO₂ have been, and will be, selected as the reservoir, which makes it difficult to predict scientifically possible leak rates. We overview leak rates used or estimated in previous studies and set the leak rates based on them in the following subsection.

Leak rate

Various leak rates have been used in simulations of leaked CO₂ dispersion in the sea. Many of those studies (*e.g.*, [3,12,13,32]) referred to 3,800 tonnes/y, the maximal seepage rate estimated in an enhanced oil recovery site, Rangely in USA [33]. In addition, the rate of O(10⁵) tonnes/y was used as a 100 times treatment of the Rangely's rate (about 0.3 M tonnes/y [12]) and as a leakage through an extraordinary large fault (about 0.1 M tonnes/y [3,13]).

We consider, however, that the rate of O(10⁵) tonnes/y is too high to occur, referring to the simulations of CO₂ migration from the sub-seabed reservoir to the seabed through fractures or faults [34,35]. Assuming that a vertical fault was suddenly formed from the center of the reservoir to the seabed just after completion of 0.1 M tonnes of CO₂ injection, Nakajima *et al.* [34] showed that the maximum leak rate ranged from about 150 tonnes/y to 600 tonnes/y, depending on the assumed permeability of the fault between 0.1 and 1 Darcy. The CO₂ storage of 0.1 M tonnes is too small to refer to here, and it may be guessed that the leak rate could reach O(10⁵) tonnes/y if the stored CO₂ was much more, *e.g.*, O(10¹) M tonnes. The situation of the simulation is, however, too unrealistic; it is considered unlikely that a new fault directly connecting from the reservoir to the seabed is formed. Thus, we guess that CO₂ leak with the rate of O(10⁵) tonnes/y would hardly occur. In the Kang *et al.*'s simulation [35], on the other hand, CO₂ had been injected for 30 years into a reservoir formation with a large fault vertically running through the overburden to the seabed. The leakage rate finally reached approximately 0.4 M tonnes/y, when the injection rate was 1 M tonnes/y. However, it is unlikely that CO₂ has been injected for 30 years with the leakage undetected, and so the injection would be suspended before the leak rate became so huge. Also, Blackford *et al.* [36] speculated the leak rate through a fracture to be O(10)-O(10²) tonnes/day, namely,

$O(10^3)$ - $O(10^4)$ tonnes/y.

Based on the consideration above, 2 leakage rates were assumed in the present study: 1,000 and 10,000 tonnes/y. Although dissolved CO₂ affects seawater density, it was reported that CO₂ released in the sea does not lead to vertical movement of seawater if CO₂ concentration is lower than 0.02–0.03 kg/m³ [37]. This value is equivalent of 2–3 $\times 10^{-9}$ 1/m³ of the tracer concentration when the leakage rate is 10,000 tonnes/y, and is an order of magnitude larger than the result shown in Fig. 3. It is, thus, unnecessary to take the vertical movement due to CO₂ concentration into consideration.

Vertical flow is produced by bubble plumes. It is, however, not considered in this study because the resolution is coarse and also because the model is a hydrostatic model. To explicitly resolve the vertical flow, it is necessary to use a non-hydrostatic model with a finer resolution [3,13].

Biological impact threshold

To set thresholds of biological impacts, we compiled data of the median lethal dose (LD₅₀) of ΔpCO₂ and the median lethal time (LT₅₀) from papers studying mortality rates of organisms due to CO₂ increase in seawater (Fig. 4). When LD₅₀ and LT₅₀ were not explicitly described in the papers, we calculated them with the Probit Analysis [38], or interpolated or assumed them from the mortality data or graphs in the papers. The compiled data set consists of 6 species of fish (56 data [39–41]), 14 species of crustacean (29 data [42–51]), 4 species of mollusk (shellfish and cephalopod; 4 data [39,52–55]), and a species of echinoderm (1 datum [55]).

Based on the data, which show a negative correlation between ΔpCO₂ and exposure time (Fig. 4), we set 4 thresh-

olds; Th.1: ΔpCO₂ = 13,000 μatm regardless of exposure time, Th.2: ΔpCO₂ = 2,500 μatm with the exposure of 60 hours, Th.3: ΔpCO₂ = 1,200 μatm with the exposure of 28 days, and Th.4: ΔpCO₂ = 200 μatm with the exposure of about 160 days (Fig. 4). The exposure time means a continuous exposure, but we applied it to the average over time. As a result, the thresholds are the followings: Th.2 is 2,500 μatm for the 60 hour mean of ΔpCO₂, Th.3 is 1,200 μatm for the 28 day mean, and Th.4 is 200 μatm for the 160 day mean.

RESULTS AND DISCUSSION

Tracer concentration

The tracers were advected both eastward and westward depending on the month or the season (Fig. 5); roughly speaking, the tracers were dispersed mainly westward along the coast before August, and eastward after that. The distribution of tracers was roughly consistent with the seasonal variation of the coastal flows in Hidaka Bay [15,56]. Figure 5 also shows that tracer's concentration dramatically declined away from the release point (see the white lines in the figures). The tracer concentration was the highest at the release grid cell, although the concentration at other cells instantaneously, but very rarely, became higher than the release cell. Thus, the release cell is focused on hereafter.

The seasonal variation of the concentration at the release point was great (Fig. 6). While the concentration near the bottom was relatively high in summer and fall (from May to around November), it was low in winter (from around November to February), as is also shown in Fig. 3a. Correspondingly, the concentration near the sea surface was extremely low in summer and fall, and higher in winter. This

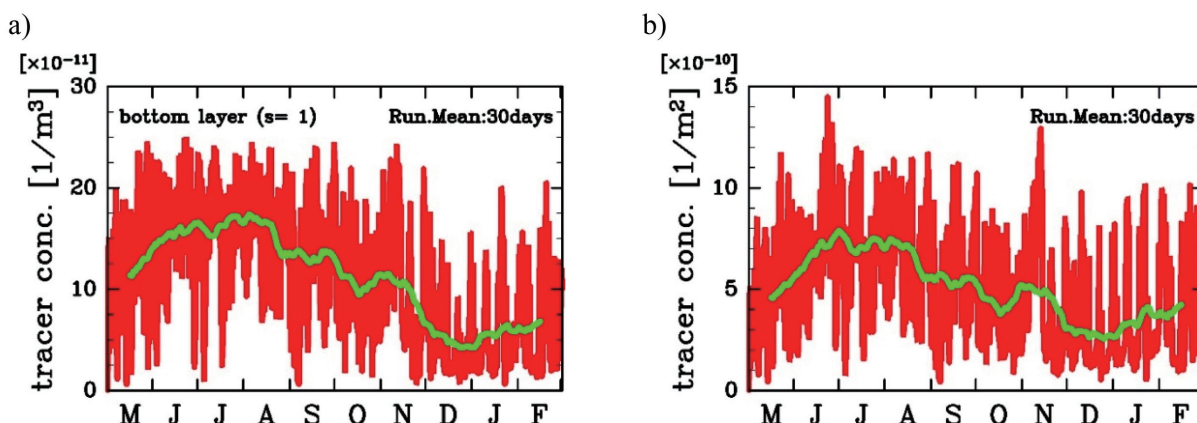


Fig. 3 Time series of the concentration at the release grid cell (a) and its vertical integral (b) of dye01 (red) and their 30 day running mean (green).

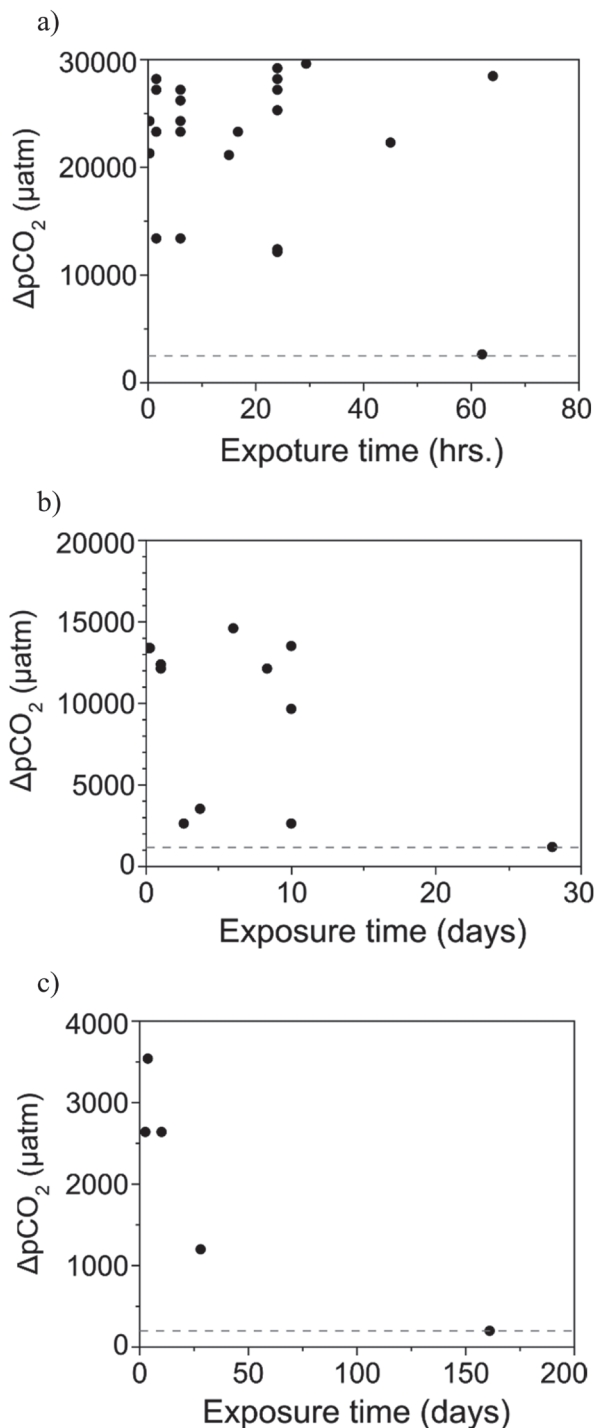


Fig. 4 Median lethal dose (LD₅₀) or median lethal time (LT₅₀) on an exposure time vs. $\Delta p\text{CO}_2$ plane. Exposure time ranges are less than 80 hours (a), 30 days (b), and 200 days (c), respectively. The dashed lines denote 2,500 μatm (a), 1,200 μatm (b), and 200 μatm (c), respectively.

is because the water column was stratified before November and was vertically mixed after November (Fig. 7). However, the vertically integrated concentration was also lower in winter than in summer (Fig. 3b). This is not explained by the vertical mixing, but by the horizontal flows, which was stronger in winter than in summer (Fig. 8). Thus, strengths of both the vertical mixing and the horizontal flows contributed to the seasonal variation of the tracer concentration in this area.

Comparison of the concentration among the four dyes indicates that the duration of the release had little influence on the concentration at the release point. Before dye02, dye03, and dye04 began to be released, dye01 had been released for 3 months, 6 months, and 9 months, respectively. However, the time series of dye02, dye03, and dye04 were almost the same as that of dye01 of the same period (Fig. 6). The concentration of dye02 at the release grid cell became almost the same concentration as dye01 within around a week after the start of the release, and the concentration of dye03 and dye04 did within a day (Figs. 9 and 10). The difference of the concentration between dye01 and dye02, dye03 or dye04 was the maximum at another grid cell than the release cell, and the maximum difference also rapidly decreased (Fig. 10). Although total amount of the released tracer increased as time elapsed, the tracers were so thinly diluted that the concentration of the tracers hardly depended on the duration of the release at any grid cell in the model domain. That is, the tracer concentration is determined by mainly sea conditions such as the stratification strength and flows, not the duration of the release, if the release rate is the same.

Biological impacts

$\Delta p\text{CO}_2$ converted from the concentration of dye01 never exceeded any of the thresholds even when the leak rate was 10,000 tonnes/y (Fig. 11). Although the raw $\Delta p\text{CO}_2$, the 60 hour running mean, and 28 day running mean in Fig. 11b sometimes exceeded 200 μatm , 200 μatm is the threshold for the 160 day running mean (Th.4). It is noted that the tracer concentration or $\Delta p\text{CO}_2$ based on it is dependent on the model resolution, which is discussed in the next subsection.

Model resolution and biological impacts

The estimated biological impacts in the previous subsection were based on the model resolution of 1/120°. Leakage at even a much smaller rate can lead higher $\Delta p\text{CO}_2$ in the vicinity of the leak point as a matter of course; in the QICS project (a controlled sub-seabed CO₂ release experiment conducted in Scotland), for example, the maximum $\Delta p\text{CO}_2$ was around

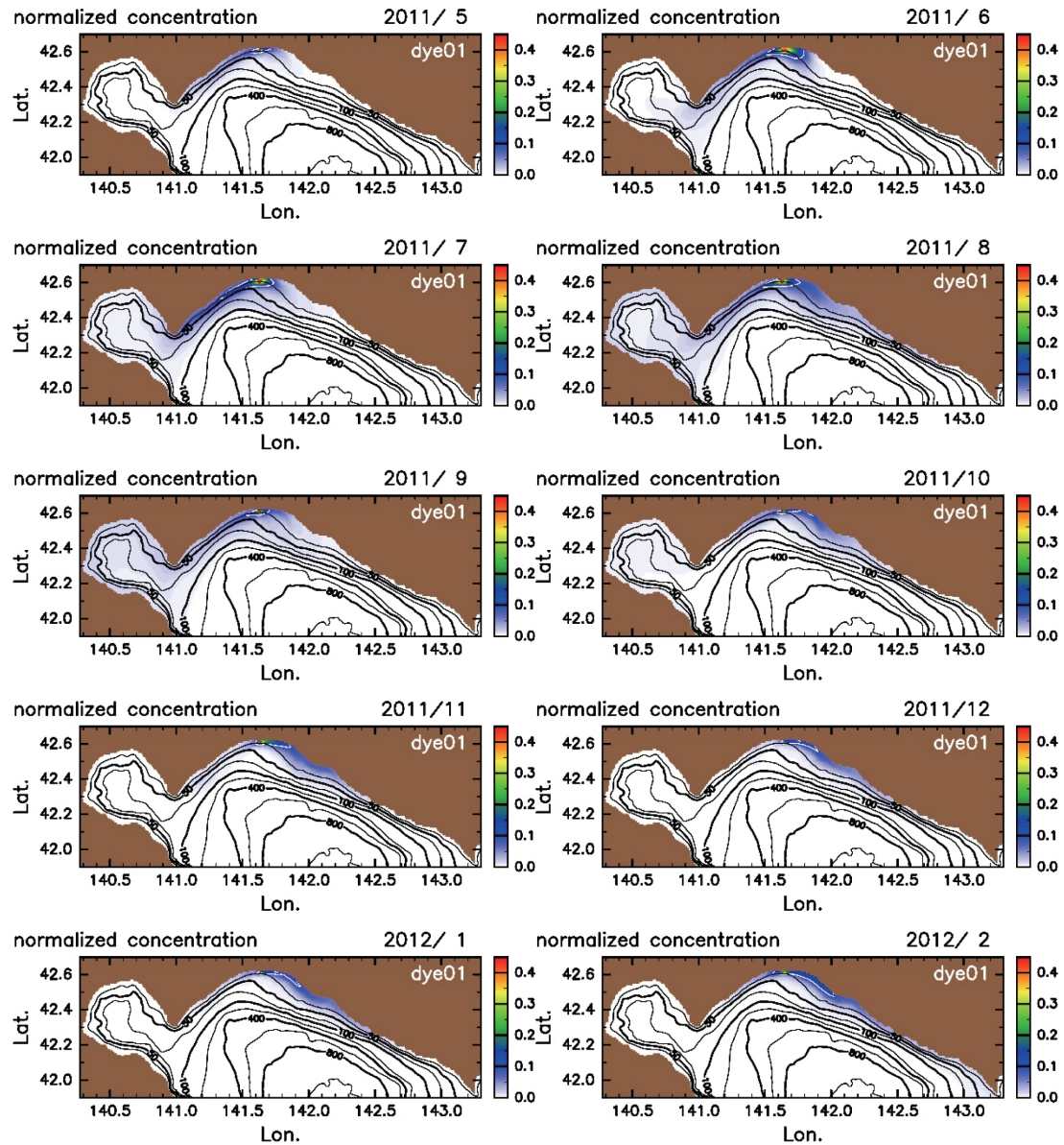


Fig. 5 Concentration of dye01 that are vertically and monthly averaged. The values are normalized by the value at the release point of July, when the concentration is the maximum. The white contour lines denote 0.1.

1,000 μatm although the maximum release rate was no more than 210 kg/day, namely about 77 tonnes/y [57]. This implies that the calculated $\Delta p\text{CO}_2$ (Fig. 11) could be underestimated, and the biological threshold might be exceeded in a smaller part of the grid cell.

It is noted, however, that this kind of underestimate is probably the case with the thresholds that depend solely on $\Delta p\text{CO}_2$ such as Th.1 but is not always the case with the thresholds that depend not only on $\Delta p\text{CO}_2$ but also on its duration such as Th.2 – Th.4. As for the latter thresholds, if

the area where a threshold is exceeded is small enough for the relevant organisms to move out within the duration, the organisms might not be impacted. Thus, in fine resolution models, all the grid cells where such thresholds are exceeded may not be regarded as biologically impacted cells. Also, even if such thresholds were exceeded in smaller part of a grid cell of coarse resolution models, it would not necessarily lead biological impacts there. The underestimate of $\Delta p\text{CO}_2$ in a coarse resolution model does not always lead to an underestimate of biological impacts. By contrast, the

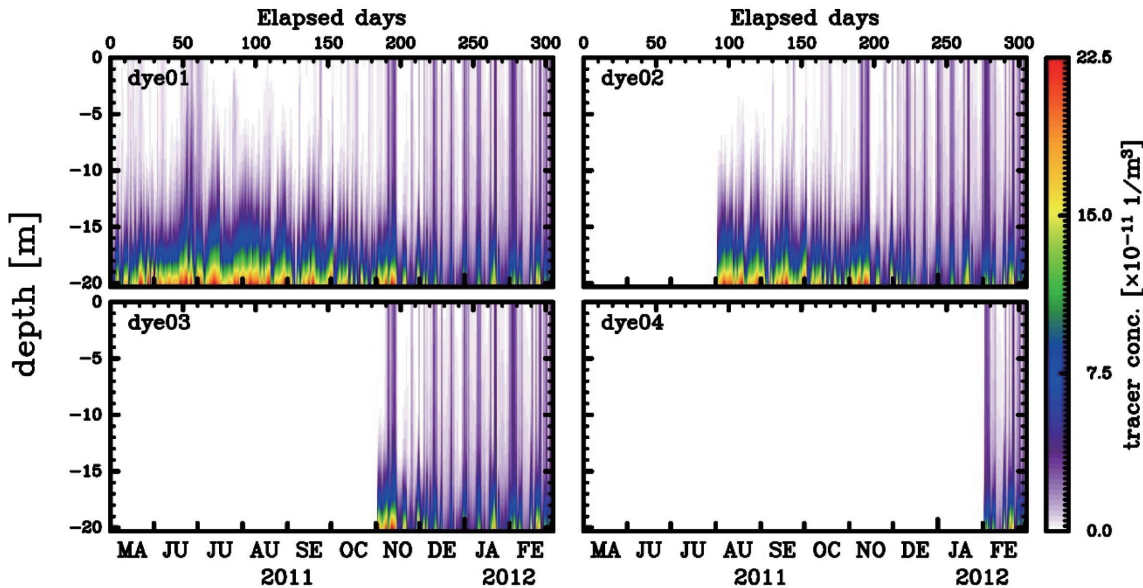


Fig. 6 Times series of the concentration of the tracers at the release point.

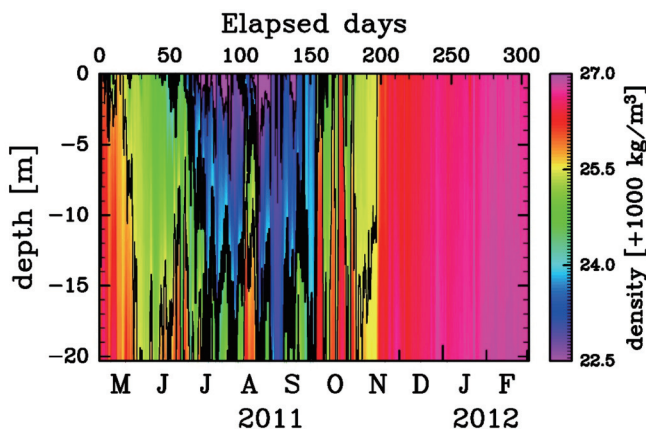


Fig. 7 Time series of the water density at the release point.

cell exceeding such thresholds in coarse resolution models like the present model may be regarded as the biologically impacted cell. Whether organisms are actually impacted in a grid cell exceeding the thresholds depends on the duration of the threshold, the grid size, and the ability to move of the potentially impacted organisms. However, at least for the PEIA, which are based on many assumptions, it is not necessarily useful to investigate these factors in detail, but the results of simulations have to be interpreted with these factors in mind in the PEIA.

Seasonality

$\Delta p\text{CO}_2$ was much higher in summer than in winter (Fig. 11). It is not only because of the stratification and weaker

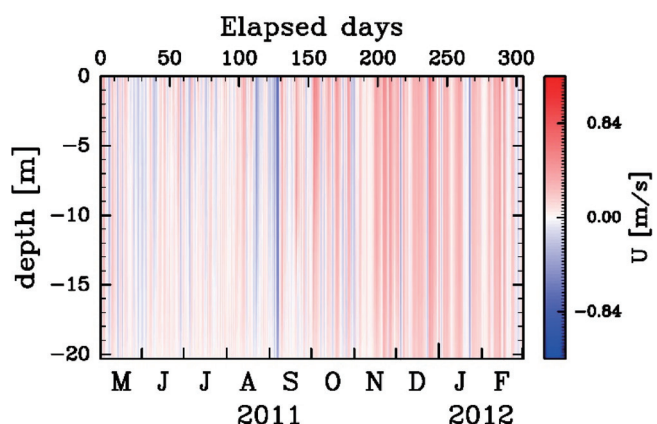


Fig. 8 Time series of the eastward velocity at the release point.

horizontal flows discussed above but also because of higher temperature in summer than in winter. Even though the DIC value (*i.e.*, the tracer concentration) is the same, $p\text{CO}_2$ value rises as temperature increases if other conditions are the same. Therefore, if the leak rate is the same, the biological impacts tend to be greater in summer than in winter.

To clarify the effects of horizontal flow, temperature and stratification, we compare the $\Delta p\text{CO}_2$ of August and December assuming that leak rate is 10,000 tonnes/y. While a $\Delta p\text{CO}_2$ value of August is calculated from the monthly-mean dye concentration, temperature, and salinity of August, the following four $\Delta p\text{CO}_2$ values of December are calculated.

Case 1: $\Delta p\text{CO}_2$ based on the monthly-mean dye01 concen-

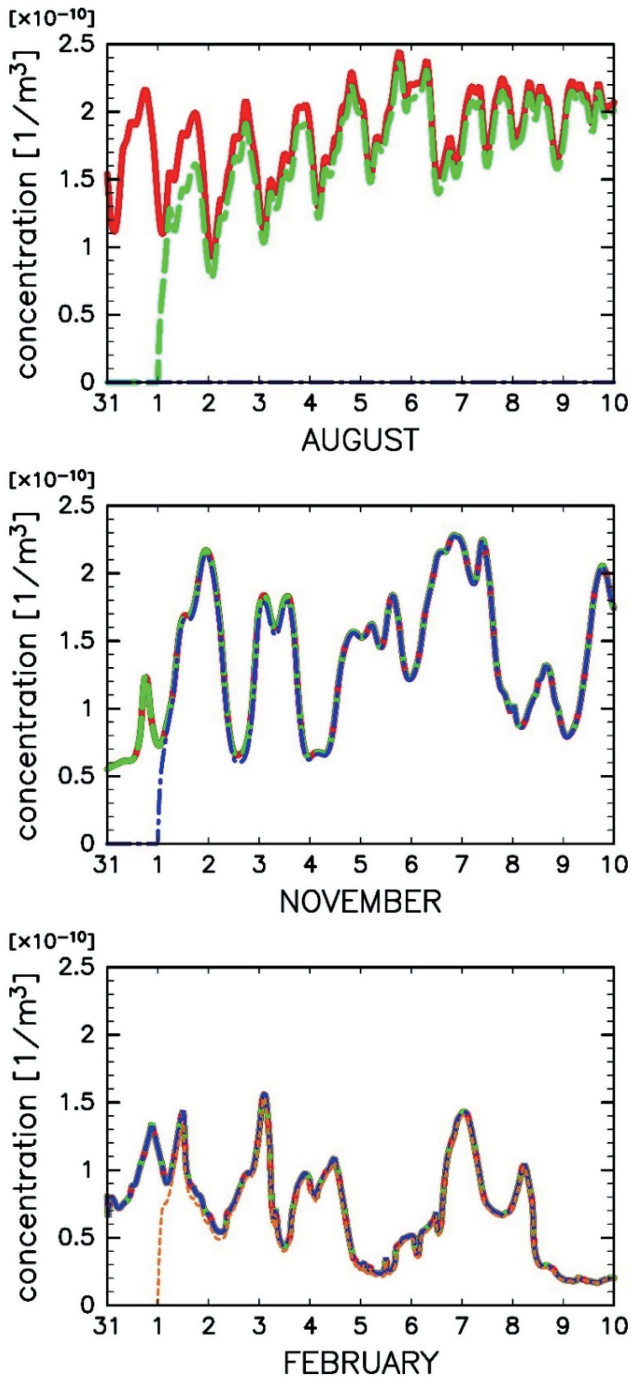


Fig. 9 Time series of the concentration of dye01 (red solid), dye02 (green broken), dye03 (blue long dashed dotted), and dye04 (orange dashed) at the release grid cell. Note that all the 4 lines are plotted in every panel although some lines are almost completely overlapped.

tration, temperature, and salinity of December.

Case 2: the same as the case 1 but the dye01 concentration of December is multiplied by 2.56, which is the ratio of the

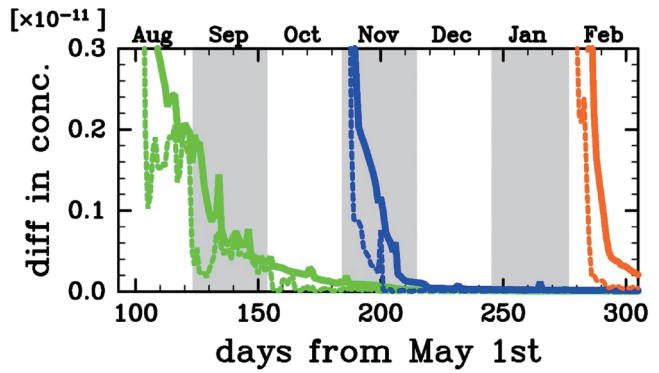


Fig. 10 Time series of the difference in the concentration between dye01 and dye02 (green), dye01 and dye03 (blue), and dye01 and dye04 (orange) at the release grid cell (dashed lines) and the cell where the difference is the maximal in the whole domain (solid lines).

monthly-mean vertically integrated dye01 concentration of August to December. Assuming that the difference of the vertically integrated dye concentrations (**Fig. 3b**) between summer and winter is due to the horizontal flows, the case 2 shows the effect of the horizontal flows.

Case 3: the same as the case 1 but the monthly-mean temperature of August is used instead of the monthly-mean temperature of December.

Case 4: ΔpCO_2 based on the dye01 concentration of December multiplied by 2.56, the monthly-mean temperature of August, and the monthly-mean salinity of December.

The difference between August and December in the case 2 is still large (**Table 2**). This indicates that ΔpCO_2 would be much larger in summer than in winter if horizontal flows in winter were weaker. The effect of temperature is relatively small (case 3). Even though the effects of the horizontal flows and temperature are eliminated (case 4), ΔpCO_2 of August is much higher than that of December, which implies that the stratification is the most significant effect on ΔpCO_2 . Thus, the results that ΔpCO_2 is larger in summer than in winter is general in all sea areas but for the areas where water column is vertically mixed throughout the year by, for example, tidal mixing.

Assumption of CO₂ bubble dissolution

In the present simulation, tracers were released in only the bottom grid cell. This may lead overestimation of ΔpCO_2 , especially in summer of the 10,000 tonnes/y case. Since the height of the bottom cell was about 2.4 m, the implicit assumption is that all the CO₂ bubbles leaked out dissolved

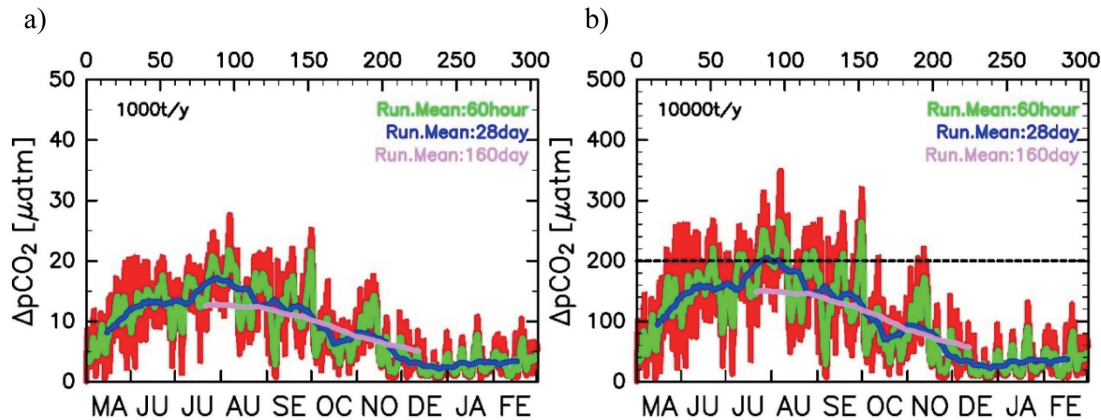


Fig. 11 Time series of ΔpCO_2 (red) and its 60 hour (green), 28 day (blue), and 160 day (pink) running mean when the leak rate is (a) 1,000 tonnes/y and (b) 10,000 tonnes/y. The dashed line denotes thresholds for the 160 day mean (Th.4): 200 μatm .

Table 2 ΔpCO_2 of August and December.

| | August [μatm] | December [μatm] |
|--------|-------------------------------|---------------------------------|
| Case 1 | 178.8 | 28.2 |
| Case 2 | 178.8 | 78.2 |
| Case 3 | 178.8 | 36.2 |
| Case 4 | 178.8 | 100.2 |

within about 2.4 m from the seabed. The assumption is not necessarily wrong as CO_2 bubbles can completely dissolve in seawater within a few meters [58]. However, the height from the seabed that CO_2 bubbles reach before they completely dissolve depends on water temperature, the initial bubble size at the seabed, the leakage rate per area and pCO_2 in the surrounding seawater (*e.g.*, [3,8]). If the leakage scenario behind the simulation is that small CO_2 bubbles leak in a relatively large area, namely low leakage rate per area, the assumption that all the CO_2 bubbles dissolve in the bottom cell may not be bad. On the contrary, the CO_2 bubbles leaked in much smaller area (*i.e.*, larger leakage rates per area) with larger initial bubble sizes would rise much higher even though the leakage rate per year was the same, and consequently leaked CO_2 in the dissolved phase would not be concentrated near the bottom but be vertically distributed more widely. In such a scenario, the maximum ΔpCO_2 could be lower than the present results. In addition, the larger the leak rate is, the higher pCO_2 in the release cell would be, which prevent CO_2 bubbles from dissolving. Thus, the present results may overestimate ΔpCO_2 , but can be regarded as the conservative result.

Implications to the simulation for PEIA and monitoring

As is discussed in the previous subsections, we have to notice that there are many implicit assumptions behind the settings of the simulation in addition to explicit assumptions such as the leakage point(s) and rate, and interpret the results based on the assumptions. The resolution of the model is also among the settings. Fine resolution models might be better for the prediction of dispersion of leaked CO_2 , should leakage actually occur. However, it may not necessarily be the case with the simulation for the PEIA, where the impact areas are roughly estimated; both models have pros and cons.

Although CO_2 could continue to leak for a long time once leakage occurred (*e.g.*, [34,36]), the period of the simulation for the PEIA would not need to be so long; probably, about a month is adequate (Figs. 9 and 10), unless the area is stagnant or a small semi-enclosed bay. The Japanese regulation requires that the season when the impact of CO_2 leakage would be the worst be selected for the simulation. Hence, it is recommended that the simulation be performed for a month of the summer season. The simulation should, however, be continued until it is clarified that Th.4 is or is not exceeded, if the ΔpCO_2 averaged in the period exceeds 200 μatm .

The Japanese regulation also requires that a CO_2 concentration index of seawater be monitored at least once a year. It should be monitored in summer, especially if pCO_2 is selected as the monitored index, as stronger stratification and higher temperature make the ΔpCO_2 in the event of CO_2 leakage far larger in summer than in winter if the leak rate is the same (Fig. 11). Even though pCO_2 is monitored in summer, to detect leakage at $O(10^3)$ tonnes/y would be

hardly possible since the natural variability range of pCO₂ in this area appears to be at least 100 μatm, even when pCO₂ is regarded as a function of dissolved oxygen [59].

Lastly, we should note that the larger the leakage rate is, the more drastically ΔpCO₂ increases because pCO₂ has an approximately exponential relation with DIC (e.g., [60]). While the leak rate increases during the injection, it rapidly decreases after the suspension of the injection [35]. Hence, the earlier CO₂ leakage could be detected during injection, the smaller biological impacts would be.

CONCLUSIONS

Keeping the PEIA for offshore CO₂ geological storage in mind, we conducted a simulation where passive tracers were released off Tomakomai in Hidaka Bay. Strong stratification and somewhat weaker flows in summer lead the tracer concentration higher in summer than winter. Also, higher temperature in summer contributed to much higher ΔpCO₂ than winter when the leak rate was the same. It was shown that the effect of the stratification is the largest of the three, and, therefore, this result is general, not specific to off Tomakomai. Thus, it is suggested that a simulation of dispersion of leaked CO₂ for the PEIA be conducted for summer, and that monitoring of pCO₂ (or another CO₂ concentration index) also be conducted in summer if it is conducted once a year.

To assess biological impacts, biological impacts data for ΔpCO₂ were newly compiled and biological impact thresholds were established. Generally, biological impacts depend not only on ΔpCO₂ but also on its duration. Even though ΔpCO₂ exceeds a threshold that also depends on the duration in a grid cell, the cell may not be regarded as the biologically impacted cell, especially when the model resolution is fine. A simulation for the PEIA is conducted based on many implicit and explicit assumptions (e.g., leak rates, leak points, CO₂ bubble dissolution, and so on). It is important to clarify the assumptions and to interpret simulation results based on the assumptions.

ACKNOWLEDGEMENTS

This paper was based on results obtained from a project (JPNP18006) commissioned by the New Energy and Industrial Technology Development Organization (NEDO) and the Ministry of Economy, Trade and Industry (METI) of Japan. Numerical simulations were performed by the super computer system of CRIEPI (HPE SGI 8600) under a joint research agreement between RITE and CRIEPI. Data

analysis was done on the Institute of Low Temperature Science Information System, Hokkaido University. Tidal data of TOMAKOMAI-NISHIKO were downloaded from JODC Data On-line Service System (J-DOSS; <https://www.jodc.go.jp/jodcweb/index.html>). Figures were produced by GFD-DENNOU Library (<https://www.gfd-dennou.org/index.html.en>). This paper improved greatly thanks to anonymous reviewers.

REFERENCES

- [1] Friedlingstein P, O'Sullivan M, Jones MW, Andrew RM, Hauck J, Olsen A, Peters GP, Peters W, Pongratz J, Sitch S, Le Quéré C, Canadell JG, Ciais P, Jackson RB, Alin S, Aragão LEOC, Arneth A, Arora V, Bates NR, Becker M, Benoit-Cattin A, Bittig HC, Bopp L, Bultan S, Chandra N, Chevallier F, Chini LP, Evans W, Florentie L, Forster PM, Gasser T, Gehlen M, Gilfillan D, Gkrizalis T, Gregor L, Gruber N, Harris I, Hartung K, Haverd V, Houghton RA, Ilyina T, Jain AK, Joetzjer E, Kadono K, Kato E, Kitidis V, Korsbakken JI, Landschützer P, Lefèvre N, Lenton A, Lienert S, Liu Z, Lombardozzi D, Marland G, Metzl N, Munro DR, Nabel JEMS, Nakaoka SI, Niwa Y, O'Brien K, Ono T, Palmer PI, Pierrot D, Poulter B, Resplandy L, Robertson E, Rödenbeck C, Schwinger J, Séférian R, Skjelvan I, Smith AJP, Sutton AJ, Tanhua T, Tans PP, Tian H, Tilbrook B, van der Werf G, Vuchard N, Walker AP, Wanninkhof R, Watson AJ, Willis D, Wiltshire AJ, Yuan W, Yue X, Zaehle S: Global carbon budget 2020. *Earth Syst. Sci. Data*, **12**(4), 3269–3340, 2020. <https://doi.org/10.5194/essd-12-3269-2020>
- [2] IEA: Energy Technology Perspectives 2017: Catalysing Energy Technology Transformations. IEA, Paris, France, 2017. https://doi.org/10.1787/energy_tech-2017-en
- [3] Jeong SM, Ko S, Sean WY: Numerical prediction of the behavior of CO₂ bubbles leaked from seafloor and their convection and diffusion near southeastern coast of Korea. *Appl. Sci. (Basel)*, **10**(12), 4237, 2020. <https://doi.org/10.3390/app10124237>
- [4] Ringrose PS, Meckel TA: Maturing global CO₂ storage resources on offshore continental margins to achieve 2DS emissions reductions. *Sci. Rep.*, **9**(1), 17944, 2019. PMID:31784589 <https://doi.org/10.1038/s41598-019-54363-z>

- [5] Johnsson F, Reiner D, Itaoka K, Herzog H: Stakeholder attitudes on carbon capture and storage—an international comparison. *Int. J. Greenh. Gas Control*, **4**(2), 410–418, 2010. <https://doi.org/10.1016/j.ijggc.2009.09.006>
- [6] Paluszny A, Graham CC, Daniels KA, Tsaparli V, Xenias D, Salimzadeh S, Whitmarsh L, Harrington JF, Zimmerman RW: Caprock integrity and public perception studies of carbon storage in depleted hydrocarbon reservoirs. *Int. J. Greenh. Gas Control*, **98**, 103057, 2020. <https://doi.org/10.1016/j.ijggc.2020.103057>
- [7] Metz B, Davidson O, De Coninck HC, Loos M, Meyer L: IPCC Special Report on Carbon Dioxide Capture and Storage. Cambridge University Press, Cambridge, UK, 2005.
- [8] Dewar M, Sellami N, Chen B: Dynamics of rising CO₂ bubble plumes in the QICS field experiment: Part 2—Modelling. *Int. J. Greenh. Gas Control*, **38**, 52–63, 2015. <https://doi.org/10.1016/j.ijggc.2014.11.003>
- [9] Dixon T, McCoy ST, Havercroft I: Legal and regulatory developments on CCS. *Int. J. Greenh. Gas Control*, **40**, 431–448, 2015. <https://doi.org/10.1016/j.ijggc.2015.05.024>
- [10] Yanagi K, Nakamura A, Komatsu E: The importance of designing a comprehensive strategic environmental assessment (SEA) & environmental impact assessment (EIA) for carbon capture and storage in Japan. *Int. J. Greenh. Gas Control*, **91**, 102823, 2019. <https://doi.org/10.1016/j.ijggc.2019.102823>
- [11] Nakamura K: Legal issues on environmental impact assessment for CCS. *Hogaku Kenkyu Ronshu*, **50**, 63–79, 2019. [In Japanese]
- [12] Blackford JC, Jones N, Proctor R, Holt J: Regional scale impacts of distinct CO₂ additions in the North Sea. *Mar. Pollut. Bull.*, **56**(8), 1461–1468, 2008. PMID:18579160 <https://doi.org/10.1016/j.marpolbul.2008.04.048>
- [13] Kano Y, Sato T, Kita J, Hirabayashi S, Tabeta S: Multi-scale modeling of CO₂ dispersion leaked from seafloor off the Japanese coast. *Mar. Pollut. Bull.*, **60**(2), 215–224, 2010. PMID:19853873 <https://doi.org/10.1016/j.marpolbul.2009.09.024>
- [14] Phelps JJC, Blackford JC, Holt JT, Polton JA: Modelling large-scale CO₂ leakages in the North Sea. *Int. J. Greenh. Gas Control*, **38**, 210–220, 2015. <https://doi.org/10.1016/j.ijggc.2014.10.013>
- [15] Rosa AL, Isoda Y, Kobayashi N: Seasonal variations of shelf circulation in Hidaka Bay, Hokkaido, Japan, with an interpretation of the migration route of juvenile walleye pollock. *J. Oceanogr.*, **65**(5), 615–626, 2009. <https://doi.org/10.1007/s10872-009-0052-6>
- [16] Shimizu M, Isoda Y: Flow structure of the coastal Oyashio on the shelf area of Hidaka Bay. *Bull. Coastal Oceanography*, **36**, 163–169, 1999. [in Japanese with English abstract] https://doi.org/10.32142/engankaiyo.36.2_163
- [17] Lessin G, Artioli Y, Queirós AM, Widdicombe S, Blackford JC: Modelling impacts and recovery in benthic communities exposed to localised high CO₂. *Mar. Pollut. Bull.*, **109**(1), 267–280, 2016. PMID:27289279 <https://doi.org/10.1016/j.marpolbul.2016.05.071>
- [18] Shchepetkin AF, McWilliams JC: The regional oceanic modeling system (ROMS): a split-explicit, free-surface, topography-following-coordinate oceanic model. *Ocean Model. (Oxf.)*, **9**(4), 347–404, 2005. <https://doi.org/10.1016/j.ocemod.2004.08.002>
- [19] Tsumune D, Tsubono T, Aoyama M, Uematsu M, Misumi K, Maeda Y, Yoshida Y, Hayami H: One-year, regional-scale simulation of ¹³⁷Cs radioactivity in the ocean following the Fukushima Dai-ichi Nuclear Power Plant accident. *Biogeosciences*, **10**(8), 5601–5617, 2013. <https://doi.org/10.5194/bg-10-5601-2013>
- [20] Smolarkiewicz PK, Margolin LG: MPDATA: A finite-difference solver for geophysical flows. *J. Comput. Phys.*, **140**(2), 459–480, 1998. <https://doi.org/10.1006/jcph.1998.5901>
- [21] Large WG, McWilliams JC, Doney SC: Oceanic vertical mixing: A review and a model with a nonlocal boundary layer parameterization. *Rev. Geophys.*, **32**(4), 363–403, 1994. <https://doi.org/10.1029/94RG01872>
- [22] Miyazawa Y, Zhang R, Guo X, Tamura H, Ambe D, Lee JS, Okuno A, Yoshinari H, Setou T, Komatsu K: Water mass variability in the western North Pacific detected in a 15-year eddy resolving ocean reanalysis. *J. Oceanogr.*, **65**(6), 737–756, 2009. <https://doi.org/10.1007/s10872-009-0063-3>
- [23] Hashimoto A, Hirakuchi H, Toyoda Y, Nakaya K: Prediction of regional climate change over Japan due to global warming (Part 1)—Evaluation of numerical weather forecasting and analysis system (NuWFAS) applied to a long-term climate simulation. CRIEPI report, N10044, Central Research Institute of Electric Power Industry, Tokyo, Japan, 2010. [in Japanese with English abstract]

- [24] Toyoda Y, Hirakuchi H: Development of hydrological model with meteorological forecast model—An application to typhoon case attacked to a Kyushu distinct. CRIEPI report, N08058, Central Research Institute of Electric Power Industry, Tokyo, Japan, 2009. [in Japanese with English abstract]
- [25] Egbert GD, Erofeeva SY: Efficient inverse modeling of barotropic ocean tides. *J. Atmos. Ocean. Technol.*, **19**(2), 183–204, 2002. [https://doi.org/10.1175/1520-0426\(2002\)019<0183:EIMOBO>2.0.CO;2](https://doi.org/10.1175/1520-0426(2002)019<0183:EIMOBO>2.0.CO;2)
- [26] Kikkawa T, Kita J, Ishimatsu A: Comparison of the lethal effect of CO₂ and acidification on red sea bream (*Pagrus major*) during the early developmental stages. *Mar. Pollut. Bull.*, **48**(1–2), 108–110, 2004. PMID:14725881 [https://doi.org/10.1016/S0025-326X\(03\)00367-9](https://doi.org/10.1016/S0025-326X(03)00367-9)
- [27] Orr JC, Epitalon JM: Improved routines to model the ocean carbonate system: mocsy 2.0. *Geosci. Model Dev.*, **8**(3), 485–499, 2015. <https://doi.org/10.5194/gmd-8-485-2015>
- [28] Lueker TJ, Dickson AG, Keeling CD: Ocean pCO₂ calculated from dissolved inorganic carbon, alkalinity, and equations for K_1 and K_2 : Validation based on laboratory measurements of CO₂ in gas and seawater at equilibrium. *Mar. Chem.*, **70**(1–3), 105–119, 2000. [https://doi.org/10.1016/S0304-4203\(00\)00022-0](https://doi.org/10.1016/S0304-4203(00)00022-0)
- [29] Dickson AG, Riley JP: The estimation of acid dissociation constants in seawater media from potentiometric titrations with strong base. I. The ionic product of water — K_w . *Mar. Chem.*, **7**(2), 89–99, 1979. [https://doi.org/10.1016/0304-4203\(79\)90001-X](https://doi.org/10.1016/0304-4203(79)90001-X)
- [30] Ministry of the Environment: Results of Fall Survey in Tomakomai Offshore, FY 2019, collection of figures and tables. https://www.env.go.jp/water/31_lautumn_appendix.pdf [accessed on March 30, 2023]
- [31] Taguchi F, Fujiwara T, Yamada Y, Fujita K, Sugiyama M: Alkalinity in coastal seas around Japan. *Bull. Coast. Oceanogr.*, **47**, 71–75, 2009. [in Japanese with English abstract] https://doi.org/10.32142/engankaiyo.47.1_71
- [32] Sakaizawa R, Kawai T, Sato T, Oyama H, Tsumune D, Tsubono T, Goto K: The inclusion of ocean-current effects in a tidal-current model as forcing in the convection term and its application to the mesoscale fate of CO₂ seeping from the seafloor. *Ocean Model. (Oxf.)*, **123**, 40–54, 2018. <https://doi.org/10.1016/j.ocemod.2018.01.001>
- [33] Klusman RW: Rate measurements and detection of gas microseepage to the atmosphere from an enhanced oil recovery/sequestration project, Rangely, Colorado, USA. *Appl. Geochem.*, **18**(12), 1825–1838, 2003. [https://doi.org/10.1016/S0883-2927\(03\)00108-2](https://doi.org/10.1016/S0883-2927(03)00108-2)
- [34] Nakajima T, Xue Z, Chiyonobu S, Azuma H: Numerical simulation of CO₂ leakage along fault system for the assessment of environmental impacts at CCS site. *Energy Procedia*, **63**, 3234–3241, 2014. <https://doi.org/10.1016/j.egypro.2014.11.350>
- [35] Kang K, Huh C, Kang SG: A numerical study on the CO₂ leakage through the fault during offshore carbon sequestration. *Journal of the Korean Society for Marine Environment and Energy*, **18**(2), 94–101, 2015. [in Korean with English abstract] <https://doi.org/10.7846/JKOSMEE.2015.18.2.94>
- [36] Blackford J, Haeckel M, Wallmann K: Report on range of long-term scenarios to be simulated. Deliverable Number D12.2, WP12/CCT2; lead beneficiary number 2, 2012. https://doi.org/10.3289/ECO2_D12.2
- [37] Masuda Y, Yamanaka Y, Sasai Y: Optimization of the horizontal shape of CO₂ injected domain and the depths of release in moving-ship type CO₂ ocean sequestration. *J. Mar. Sci. Technol.*, **18**(2), 220–228, 2013. <https://doi.org/10.1007/s00773-012-0202-1>
- [38] Finney DJ: Probit Analysis: A Statistical Treatment of the Sigmoid Response Curve. Cambridge University Press, Cambridge, UK, 1952.
- [39] Kikkawa T, Ishimatsu A, Kita J: Acute CO₂ tolerance during the early developmental stages of four marine teleosts. *Environ. Toxicol.*, **18**(6), 375–382, 2003. PMID:14608607 <https://doi.org/10.1002/tox.10139>
- [40] Kikkawa T, Hasegawa K, Minowa Y, Setoguma T, Kita J: CO₂ tolerance of tomato clownfish (*Amphiprion frenatus*) eggs. *Rep. Mar. Ecol. Res. Inst.*, **9**, 47–54, 2006. [in Japanese with English abstract]
- [41] Ishimatsu A, Kojima Y, Hayashi M: Effects of CO₂ ocean sequestration on deep-sea animals. OCEANS 2008 – MTS/IEEE Kobe Techno-Ocean, Kobe, Japan, pp. 1–4, 2008. <https://doi.org/10.1109/OCEANSKO-BE.2008.4531034>
- [42] Pascal PY, Fleeger JW, Galvez F, Carman KR: The toxicological interaction between ocean acidity and metals in coastal meiobenthic copepods. *Mar. Pollut. Bull.*, **60**(12), 2201–2208, 2010. PMID:20875652 <https://doi.org/10.1016/j.marpolbul.2010.08.018>

- [43] Kikkawa T, Watanabe Y, Katayama Y, Kita J, Ishimatsu A: Acute CO₂ tolerance limits of juveniles of three marine invertebrates, *Sepia lycidas*, *Sepioteuthis lessoniana*, and *Marsupenaeus japonicus*. *Plankton Benthos Res.*, **3**(3), 184–187, 2008. <https://doi.org/10.3800/pbr.3.184>
- [44] Watanabe Y, Yamaguchi A, Ishida H, Harimoto T, Suzuki S, Sekido Y, Ikeda T, Shirayama Y, Takahashi MM, Ohsumi T, Ishizaka J: Lethality of increasing CO₂ levels on deep-sea copepods in the western North Pacific. *J. Oceanogr.*, **62**(2), 185–196, 2006. <https://doi.org/10.1007/s10872-006-0043-9>
- [45] Bechmann RK, Taban IC, Westerlund S, Godal BF, Arnberg M, Vingen S, Ingvarsdotir A, Baussant T: Effects of ocean acidification on early life stages of shrimp (*Pandalus borealis*) and mussel (*Mytilus edulis*). *J. Toxicol. Environ. Health A*, **74**(7–9), 424–438, 2011. PMID:21391089 <https://doi.org/10.1080/1528739.2011.550460>
- [46] Dissanayake A, Ishimatsu A: Synergistic effects of elevated CO₂ and temperature on the metabolic scope and activity in a shallow-water coastal decapod (*Metapenaeus joyneri*; Crustacea: Penaeidae). *ICES J. Mar. Sci.*, **68**(6), 1147–1154, 2011. <https://doi.org/10.1093/icesjms/fsq188>
- [47] Zhang D, Li S, Wang G, Guo D: Impacts of CO₂-driven seawater acidification on survival, egg production rate and hatching success of four marine copepods. *Acta Oceanol. Sin.*, **30**(6), 86–94, 2011. <https://doi.org/10.1007/s13131-011-0165-9>
- [48] Kurihara H, Matsui M, Furukawa H, Hayashi M, Ishimatsu A: Long-term effects of predicted future seawater CO₂ conditions on the survival and growth of the marine shrimp *Palaemon pacificus*. *J. Exp. Mar. Biol. Ecol.*, **367**(1), 41–46, 2008. <https://doi.org/10.1016/j.jembe.2008.08.016>
- [49] Long WC, Swiney KM, Harris C, Page HN, Foy RJ: Effects of ocean acidification on juvenile red king crab (*Paralithodes camtschaticus*) and Tanner crab (*Chionoecetes bairdi*) growth, condition, calcification, and survival. *PLoS One*, **8**(4), e60959, 2013. PMID:23593357 <https://doi.org/10.1371/journal.pone.0060959>
- [50] Sato T, Watanabe Y, Toyota K, Ishizaka J: Extended probit mortality model for zooplankton against transient change of PCO₂. *Mar. Pollut. Bull.*, **50**(9), 975–979, 2005. PMID:15913663 <https://doi.org/10.1016/j.marpolbul.2005.04.003>
- [51] Basallote MD, De Orte MR, DelValls TA, Riba I: Studying the effect of CO₂-induced acidification on sediment toxicity using acute amphipod toxicity test. *Environ. Sci. Technol.*, **48**(15), 8864–8872, 2014. PMID:24988484 <https://doi.org/10.1021/es5015373>
- [52] Zippay ML, Hofmann GE: Effect of pH on gene expression and thermal tolerance of early life history stages of red abalone (*Haliotis rufescens*). *J. Shellfish Res.*, **29**(2), 429–439, 2010. <https://doi.org/10.2983/035.029.0220>
- [53] Talmage SC, Gobler CJ: Effects of elevated temperature and carbon dioxide on the growth and survival of larvae and juveniles of three species of northwest Atlantic bivalves. *PLoS One*, **6**(10), e26941, 2011. PMID:22066018 <https://doi.org/10.1371/journal.pone.0026941>
- [54] Watson SA, Southgate PC, Miller GM, Moorhead JA, Knauer J: Ocean acidification and warming reduce juvenile survival of the fluted giant clam, *Tridacna squamosa*. *Molluscan Res.*, **32**, 177–180, 2012.
- [55] Shirayama Y, Thornton H: Effect of increased atmospheric CO₂ on shallow water marine benthos. *J. Geophys. Res. Oceans*, **110**, C09S08, 2005. <https://doi.org/10.1029/2004JC002618>
- [56] Rosa AL, Isoda Y, Uehara K, Aiki T: Seasonal variations of water system distribution and flow patterns in the southern sea area of Hokkaido, Japan. *J. Oceanogr.*, **63**(4), 573–588, 2007. <https://doi.org/10.1007/s10872-007-0051-4>
- [57] Atamanchuk D, Tengberg A, Aleynik D, Fietzek P, Shitashima K, Lichtschlag A, Hall POJ, Stahl H: Detection of CO₂ leakage from a simulated sub-seabed storage site using three different types of pCO₂ sensors. *Int. J. Greenh. Gas Control*, **38**, 121–134, 2015. <https://doi.org/10.1016/j.ijgge.2014.10.021>
- [58] Uchimoto K, Nishimura M, Watanabe Y, Xue Z: An experiment revealing the ability of a side-scan sonar to detect CO₂ bubbles in shallow seas. *Greenh. Gases Sci. Technol.*, **10**(3), 591–603, 2020. <https://doi.org/10.1002/ghg.1991>
- [59] Ministry of Economy, Trade and Industry (METI), New Energy and Industrial Technology Development Organization (NEDO), Japan CCS Co., Ltd. (JCCS): Report of Tomakomai CCS Demonstration Project at 300 thousand tonnes cumulative injection (“Summary Report”) – overview –, 2020. https://www.meti.go.jp/english/press/2020/pdf/0515_004a.pdf [accessed on March 30, 2023]

- [60] Kano Y, Sato T, Kita J, Hirabayashi S, Tabeta S: Model prediction on the rise of pCO₂ in uniform flows by leakage of CO₂ purposefully stored under the seabed. *Int. J. Greenh. Gas Control*, **3**(5), 617–625, 2009. <https://doi.org/10.1016/j.ijggc.2009.03.004>
- [61] Smith WHF, Sandwell DT: Global sea floor topography from satellite altimetry and ship depth soundings. *Science*, **277**(5334), 1956–1962, 1997. <https://doi.org/10.1126/science.277.5334.1956>